Methods for Benchmarking Photolithography Simulators: Part IV

Trey Graves[a], Mark D. Smith[a], and Chris A. Mack[b]

[a] KLA-Tencor Corp.,
[b] lithoguru.com

ABSTRACT

In a previous series of papers, we proposed benchmarks for lithography simulators drawn from the optics literature for aerial image, optical film-stack calculations, and mask topography effects. We extend this work and present benchmarks for PEB and resist development. These benchmarks can easily be applied to any lithography simulator that models these lithographic effects.

Keywords: Lithography simulation, numerical accuracy, calculus of variations, post-exposure bake, development, PROLITH

1. INTRODUCTION

Numerical simulation has become an essential tool in photolithographic engineering. Simulators are used in optimization of source shapes and film stacks, design for manufacturability (DFM), optical proximity correction (OPC), and more. As smaller features with even lower k1 values are printed, the accuracy of these simulators is crucial, especially if lithographers are to use these simulators to make quantitative assessments that lead to critical decision making.

The photolithographic process is made up of many independent steps (for example, imaging and PEB) that can be described by their own independent models (Fourier optics and coupled diffusion equations, respectively). It is necessary that any numerical implementation of a model in a simulator be reasonably fast, free of bugs or algorithm problems, and accurate. For these last reasons, we have extended our previous papers [1,2,3] where we proposed standard benchmark problems for aerial image calculations, image in resist calculations, and EMF mask topography effects. The benchmarks presented here are for post-exposure bake (PEB) and development models.

We will derive closed-form solutions that use the same assumptions used in the model implementation. This approach has been taken by other authors, notably Brunner [4] and Gordon [5]. These solutions can be compared against a simulator as an absolute standard. The benchmark can then be used to judge the simulator, in particular as it applies to speed vs. accuracy tradeoffs.

2. POST-EXPOSURE BAKE BENCHMARK

During PEB, the photoacid (H), created during the exposure process, diffuses through the resist and catalytically reacts with blocked polymer sites, M. At the same time, the base quencher, Q, also diffuses through the resist and neutralizes the acid [6]. Mathematically, we model this as:

$$\frac{dM}{dt} = -k_a \cdot H \cdot M \tag{1}$$

$$\frac{dH}{dt} = -k_{loss} \cdot H - k_Q \cdot H \cdot Q + D_H \nabla^2 H \tag{2}$$

Optical Microlithography XIX, edited by Donis G. Flagello, Proc. of SPIE Vol. 6154
61542X, (2006) · 0277-786X/06/$15 · doi: 10.1117/12.660031

$$\frac{dQ}{dt} = -k_Q \cdot H \cdot Q + D_Q \nabla^2 Q \,. \tag{3}$$

Here D_H is the diffusivity of the acid, k_{loss} is the acid loss reaction rate constant, k_Q is the acid-base quench rate constant, D_Q is the diffusivity of the base quencher, and k_a is the deblocking reaction rate constant.

2.1. POST-EXPOSURE BAKE SOLUTION

The neutralizing of acid and base makes an analytical solution of equations (*1*)-(3) difficult to impossible. However, a simplified solution is possible with no quencher. Setting *Q=0*, equations (*1*)-(3) reduce to two equations:

$$\frac{dM}{dt} = -k_a \cdot H \cdot M \tag{4}$$

$$\frac{dH}{dt} = -k_{loss} \cdot H + D\nabla^2 H \tag{5}$$

D now represents the diffusivity of the acid. Assuming periodic boundary conditions, the following solutions for *H* and *M* can be shown to satisfy (4) and (5):

$$H = \sum_n \hat{H}_n Cos\left(\frac{2\pi n x}{p}\right) \exp\left(-\left[\frac{2\pi n}{p}\right]^2 Dt\right) \tag{6}$$

$$M = \exp\left[-k_a \sum_n \hat{H}_n Cos\left(\frac{2\pi n x}{p}\right) \frac{1-\exp\left(-\left[\frac{2\pi n}{p}\right]^2 Dt\right)}{\left[\frac{2\pi n}{p}\right]^2 D}\right]. \tag{7}$$

x is the spatial coordinate in this 1D test problem. The pitch is labeled by *p*. $\hat{H}_n$ is the Fourier coefficient of the initial acid concentration. In the following section a solution will be derived for $\hat{H}_n$ for a specific test problem.

Another solution to (4) and (5) can be found for an infinite domain instead of periodic boundaries. The solution is obtained with a Green's function approach. This is the "resist blur" function from the IBM group [7].

2.2. POST-EXPOSURE BAKE SOLUTION VERIFICATION

To use the solution provided by (6) and (*7*) as a benchmark, we need to choose a set of conditions that give a closed-form solution for $\hat{H}_n$. The mask is alternating PSM with 90nm lines and spaces. For the imaging system, we use a 193nm exposure wavelength, NA > 0.54 (2-beam imaging with k1=0.25), coherent illumination ($\sigma = 0$), TE polarized light, and a reduction ratio = 1.0. The film stack has all optical properties set to the properties of air. The exposure dose is 25 mJ/cm^2 with the Dill C parameter set to 0.05 cm^2/mJ.

Post-exposure bake time is 90 seconds. The diffusion coefficient for acid is 10 nm^2/s. An amplification rate of 0.1 sec^{-1} is used.

With these illuminator and mask settings, the image in resist electric field *E(x)* (actually air) is

$$E(x) = E_{-1}\exp\left[-i\frac{2\pi x}{p}\right] + E_{+1}\exp\left[i\frac{2\pi x}{p}\right]. \tag{8}$$

The Fourier coefficients $E_{\pm 1} = \mp\frac{\sqrt{2}}{\pi}$ are a result of the diffraction pattern. The image in resist intensity *I* is *EE**:

$$I(x) = \frac{4}{\pi^2}\left[1-\cos\left(\frac{4\pi x}{p}\right)\right]. \tag{9}$$

The exposure model for the photoacid group concentration (denoted by [PAG]) is

$$\begin{aligned}[\mathrm{PAG}] &= \exp[-c\cdot Dose\cdot I] \\ &= \exp\left[-c\cdot Dose\cdot\frac{4}{\pi^2}\left(1-\cos\left(\frac{4\pi x}{p}\right)\right)\right]\end{aligned} \tag{10}$$

The input to PEB is the PAG concentration after the expose step, so the acid concentration

$$H = 1-[PAG] \tag{11}$$

is given by

$$H(x) = 1-\exp\left[-c\cdot Dose\cdot\frac{4}{\pi^2}\left(1-\cos\left(\frac{4\pi x}{p}\right)\right)\right]. \tag{12}$$

The solutions for *H* and *M*, equations (6) and (7), are expressed as Fourier coefficients of *H*. Taking the Fourier transform of (12), the coefficients are

$$\hat{H}_0 = \frac{1}{p}\int_0^p 1-\exp\left[-c\cdot Dose\cdot\frac{4}{\pi^2}\left(1-\cos\left(\frac{4\pi x}{p}\right)\right)\right]dx \tag{13}$$

$$\hat{H}_n = \frac{2}{p}\int_0^p \cos\left(\frac{2\pi n x}{p}\right)\left\{1-\exp\left[-c\cdot Dose\cdot\frac{4}{\pi^2}\left(1-\cos\left(\frac{4\pi x}{p}\right)\right)\right]\right\}dx. \tag{14}$$

Note that these are modified Bessel functions of the first kind, so the integrals in (13) and (14) can be written as

$$\begin{aligned}\hat{H}_0 &= 1-e^{-\Delta}I_0(\Delta) \\ \hat{H}_n &= -e^{-\Delta}I_{n/2}(\Delta) \quad n>0,\ n\ even \\ \hat{H}_n &= 0 \qquad\qquad\quad n\ odd\end{aligned}$$

where $\Delta = \frac{4 \cdot c \cdot Dose}{\pi^2}$, and $I_{n/2}$ denotes the Bessel functions [8]. Substitution of the above coefficients into equation (*7*) gives the final closed-form solution to the PEB test problem.

Figure 1 shows the L_2-norm of the blocked polymer concentration, calculated over all grid points in the simulation region. The errors are small and there is good convergence with grid size.

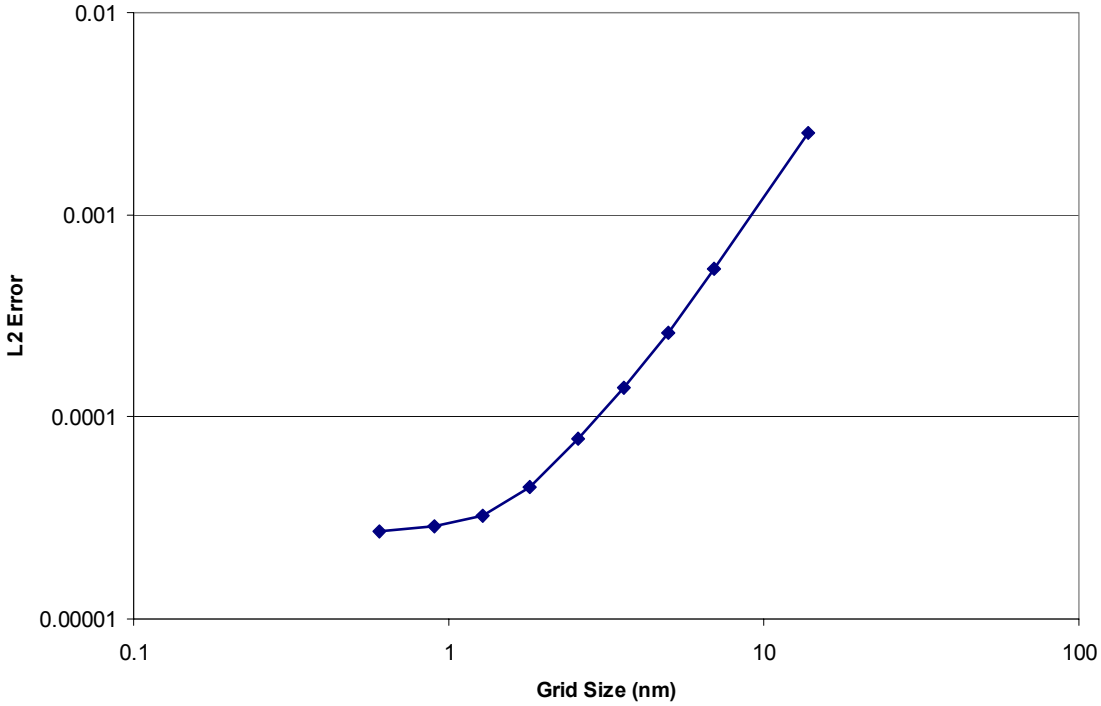

Figure 1. The L_2-norm is shown as a function of grid size. The convergence is very good. The tapering off of the error at small grid size is due to 6 digits of output in PROLITH results.

3. DEVELOP BENCHMARK

In this section, analytic solutions are derived for develop paths and develop times. These results will then be used as benchmarks to evaluate the accuracy of PROLITH's resist development model.

The developer front—defined as the border of the developer and resist at some develop time *t*— starts at the top surface of the resist. The front moves at a rate *R(x,y,z)* that is based on the amount of deblocking the polymer resin has undergone during PEB. The rate represents the scalar speed of the developer at a location *(x,y,z)* in the resist.

The develop paths are the rays that track the movement of the front; they are by this definition perpendicular to the front. The governing principle that the paths obey is the principle of least time: at a particular point in the resist, the path taken is the one that begins at the top and reaches the point the quickest. Our goal is to find the path that the developer takes. At first this may seem to be an intractable problem. There are after all an infinite number of paths that start from some location at the top of the resist and end at a point in the resist. Fortunately, the well-known mathematics of the calculus of variations provides a framework to seek a potential analytic solution [9]. As with most pencil and paper solutions, we will only be able to obtain closed-form results for a couple of special cases.

The rate R is a function of blocked polymer concentration [10]. It can also be modeled as a function of exposure dose E. Various empirical models for how R varies with E have been proposed [11]. The rate is typically a highly non-linear function of dose. By way of example, Figure 2 shows a possible develop rate distribution, and develop time contours. Three paths to a final point (y_f, z_f) are indicated. Only one of these paths (path C) is optimal.

The develop time, T_{dev}, is defined as

$$T_{dev}(y_f, z_f) = \int_{(y_0,0)}^{(y_f,z_f)} \frac{ds}{R(y(z))}. \qquad (15)$$

Here ds is the infinitesimal arc length at a point along the path. The depth variable is z; it is zero at the top of the resist and increases further into the resist. R is allowed to be an explicit function of the y coordinate only. (y will be used as the horizontal axis coordinate. Only 2D problems (y and z) will be investigated.) Expression (15) says simply that the total time to the final location (y_f, z_f) is the distance divided by speed integrated at all points along the path, starting from (y_0, 0).

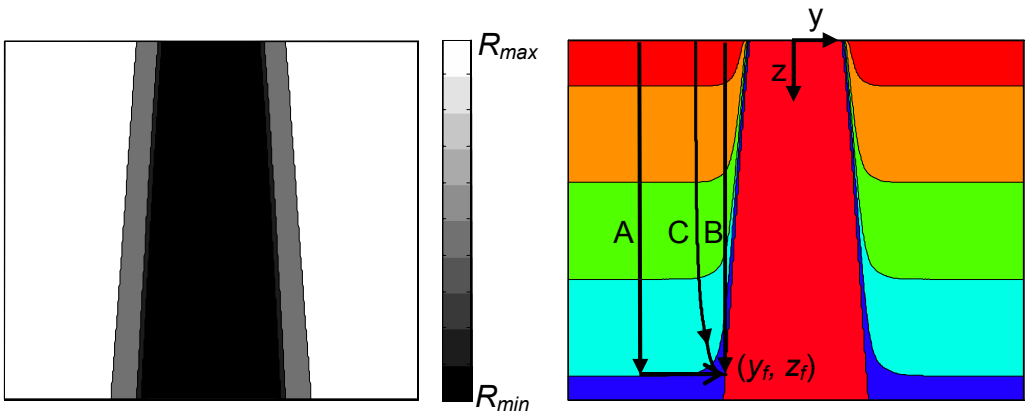

Figure 2. The plot on the left illustrates a possible develop rate as a function y and z. Note how the rate goes from R_{max} to R_{min} over a very short distance. The plot on the right shows three possible paths to the point (y_f, z_f) for the develop rate on the left. The contours represent the developer front at particular times. The middle trapezoid represents the final resist profile. Path A reaches the depth z_f the quickest, but takes too long to reach (y_f, z_f), because of the extra distance it must travel. Path B is the shortest, but the develop rate along the path is not as large as the other paths. Path C, although longer than B, takes the least amount of time to get from some point on the surface to (y_f, z_f). It is optimal because it makes the best use of distance and speed. Note that the optimal path is normal to the front.

We are interested in the determining the path $y(z)$. According to the calculus of variations, $y(z)$ satisfies the Euler-Lagrange differential equation [9],

$$F_y(z, y(z), y'(z)) - \frac{d}{dz} F_{y'}(z, y(z), y'(z)) = 0. \qquad (16)$$

F is defined as

$$F(y,y') = \frac{\sqrt{1+y'^2}}{R(y)}. \tag{17}$$

The $\sqrt{1+y'^2}$ term in *F* results from expressing *ds* using the Pythagorean Theorem in Cartesian coordinates *y* and *z*. $F_{y'}$ is the partial derivative of *F* with respect to y', where y' is *dy/dz*. If *R(y)* is not an explicit function of *z,* the Euler-Lagrange equation reduces to the Beltrami identity [9]:

$$F(y(z),y'(z)) - y'(z)F_{y'}(y(z),y'(z)) = C \tag{18}$$

C is a constant that may be determined by the boundary conditions. (It is in fact *1/R* evaluated at *z*=0.) Note that the functional T_{dev} can be now be written in terms of *F*:

$$T_{dev} = \int_{z_0}^{z_f} F(y(z),y'(z))dz\,. \tag{19}$$

Substituting *F* into the Beltrami identity gives

$$\frac{R(y)y'}{\sqrt{(1/C^2)+R^2(y)}} = 1\,,$$

which may be integrated to solve for *y(z)*:

$$\int \frac{R(y)dy}{\sqrt{(1/C^2)+R^2(y)}} = \int dz = z + B\,. \tag{20}$$

The constant *B* can be determined by boundary conditions.

Equation (20) will be our starting point for two test cases. The goal is to find suitable functional forms of *R(y)* that will allow the left hand side of equation (20) to be integrated in a closed-form manner. Furthermore, we would like to solve for *y=y(z)* and substitute this into equation (15) to give an equation for T_{dev} as a function of any location (*y*,*z*) in the resist.

3.1. LINEARLY INCREASING DEVELOP RATE

The first form for *R* that we will consider is a linear rate, symmetric about *y=0*:

$$R(y) = R_0 \frac{|y|}{y_{\max}} \tag{21}$$

R_0 is the rate constant. y_{max} is the maximum extent of the simulation region in the *+y* and *–y* direction. This rate function might occur in an LPM model [11] if the relative dose *E* is given by $E=|y|/y_{max}$ (see Figure 3) and $R=R_0E^{\gamma}$, where the develop contrast, γ, is one. Note that this an unrealistic develop rate dependence in the y direction. One reason is that the image in resist would have to have a linear dependence in *y*. For realistic cases, the image behavior usually has a quadratic or higher dependence on position (due to limited

spatial frequencies allowed through the lens and the binary nature of most masks). Also, a develop contrast of one corresponds to an unrealistically low contrast for a resist.

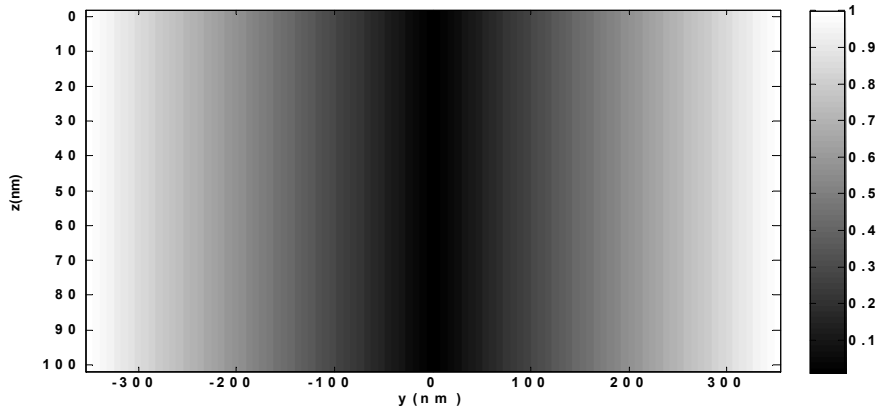

Figure 3. The exposure dose as a function of horizontal position and depth in the resist. There is no explicit z-dependence in the exposure, corresponding to infinite depth of focus and no absorption.

R is an explicit function of *y* and an implicit function of *z* (since *y=y(z)*). Let *|y|->y*. We will solve the problem for the positive *y* half-plane and mirror the solution using symmetry. This should cause no loss of generality since everywhere except the center, the develop paths will start from outside and arc down and in towards the middle of the simulation region. (This will be more obvious after the solution is found.) Only at the center are there two ways to arrive, but this is not a concern since it takes an infinite amount of time to reach the center. Substituting for *R*, we have

$$\int \frac{ydy}{\sqrt{A^2 + y^2}} = z + B$$

where $A = y_{max}/(CR_0)$. Integrating and solving for *y* gives

$$y = \sqrt{A^2 - (z + B)^2}$$

A and *B* can be determined by applying boundary conditions. In particular, the slope *dy/dz* at the top of the resist is zero; that is, $y'(z=0) = 0$. This is the so-called natural boundary condition [9]. Physically, this means the develop paths begin at time *t=0* by moving vertically down. To satisfy this boundary condition, *B* must be zero. Next, we have by definition that $y(z_f) = y_f$. This requires that

$$A^2 = y_f^2 + z_f^2 .$$

The geometry of the develop paths is therefore described by

$$y(z) = \sqrt{{y_f}^2 + {z_f}^2 - z^2} \qquad (22)$$

for $R(y)=R_0 |y|/y_{max}$. Thus, the develop paths are circles for this *R(y)*, as shown in Figure 4.

We now substitute equation (22) into equation (21), and substitute that result for *R* into equation (15). The result is that

$$T_{dev}(y_f, z_f) = \int_0^{z_f} \frac{\sqrt{1 + \dfrac{z^2}{{z_f}^2 + {y_f}^2 - z^2}}}{R_0({z_f}^2 + {y_f}^2 - z^2)^{1/2} / y_{\max}} dz \,. \tag{23}$$

After some algebraic simplification, this may be integrated to give

$$T_{dev}(y_f, z_f) = \frac{y_{\max}}{R_0} \tanh^{-1} \frac{z_f}{\sqrt{y_f^2 + z_f^2}} \,. \tag{24}$$

This may in turn be solved for y_f, which is half the CD for this particular choice of $R(y)$.

For purposes of benchmarking the PROLITH develop routine, a resist thickness of 100 nm is chosen and the CD is measured half way down. Choosing R_0=16.7 nm/s, we measure the CD at the 60 second contour so that the side wall angle is realistic. The behavior for the CD error vs. grid size is shown in Figure 5.

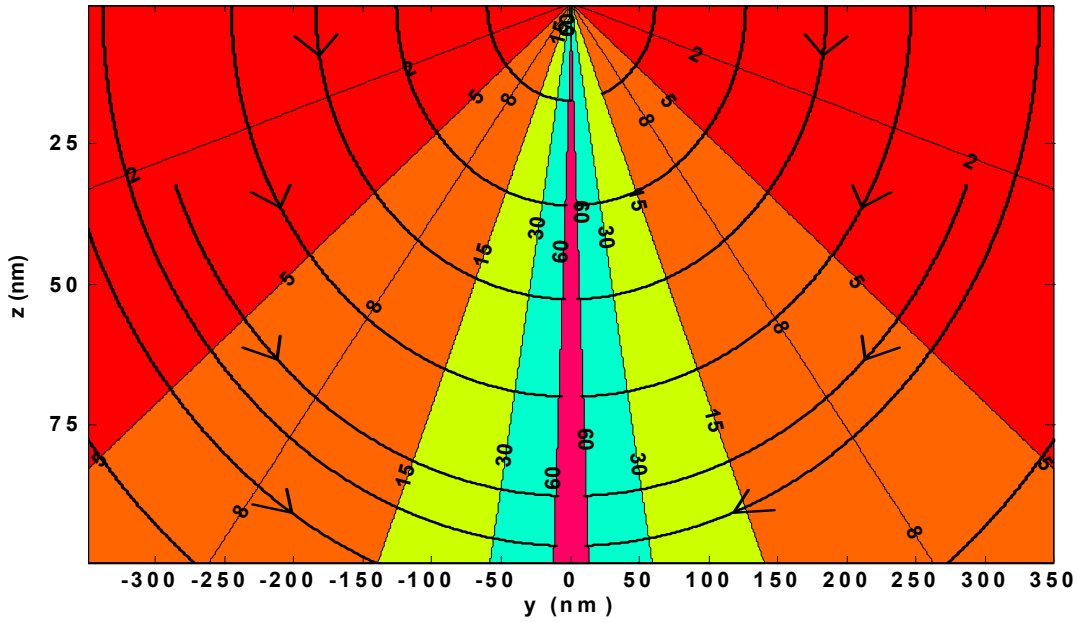

Figure 4. The develop front (contours of constant develop time) is shown for different develop times, measured in seconds, for a develop rate that is linear with position y. The parameters are R_0 = 16.7 nm/s and y_{max} = 350 nm. The resist profile is represented by the isosceles triangle at the 60 second contour.

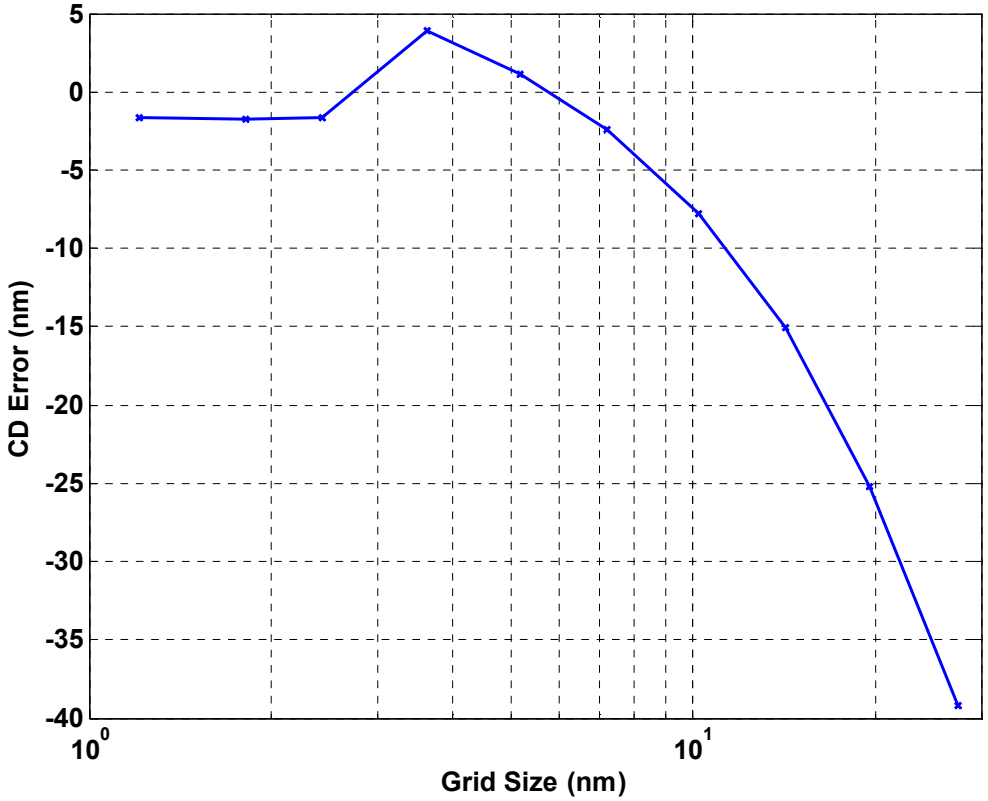

Figure 5. CD error vs. grid size for a linear develop rate in y with parameters R_0 = 16.7 nm/s and y_{max} = 350 nm.

The results indicate that PROLITH converges well with decreasing grid size. The error is large with large grid size and for small grid sizes it is under 2nm. One must keep in mind that this develop rate is very unrealistic. Still, it is an interesting case that has a simple closed-formed solution. We now move on to a develop rate that is more realistic.

3.2. EXPONENTIALLY INCREASING DEVELOP RATE

The develop rate typically changes by orders of magnitude at the mask edge. For this reason, an exponential dependency on spatial coordinate y for the develop rate is more realistic than a linear rate. Suppose in particular that the exposure dose as a function of y is given by $E(y) = e^{-sy}$ and that once again the rate is $R=R_0E^{\gamma}$. Substituting E into R gives

$$R(y) = R_0 e^{-s\gamma y} \tag{25}$$

When the contrast is large, the develop paths are mostly segmented; that is, they proceed vertical down initially, and then they move horizontally to reach the final resist profile edge.

With relation (25) for $R(y)$, the develop path to a point (y_f, z_f) can be shown, using steps similar to the case with the linear develop rate, to be:

$$y(z) = \frac{1}{\gamma s}\ln\left[\sec(s\gamma z)/\sec(s\gamma z_f)\right] + y_f \tag{26}$$

Using (15), (25), and (26), it follows that

$$T_{dev}(y_f, z_f) = \frac{e^{s\gamma y_f} \sin s\gamma z_f}{s\gamma R_0} \tag{27}$$

Because T_{dev} depends on a sinusoid, this result is only valid when $s\gamma z < \pi$. For this reason, $s\gamma = 0.38$ nm^{-1} is chosen. R_0 is set to 5.0 nm/s. The CD measurement error vs. grid size is shown in Figure 6 and the final resist profile is shown in Figure 7. The PROLITH result converges to the correct result with sub-nanometer accuracy for small grid sizes.

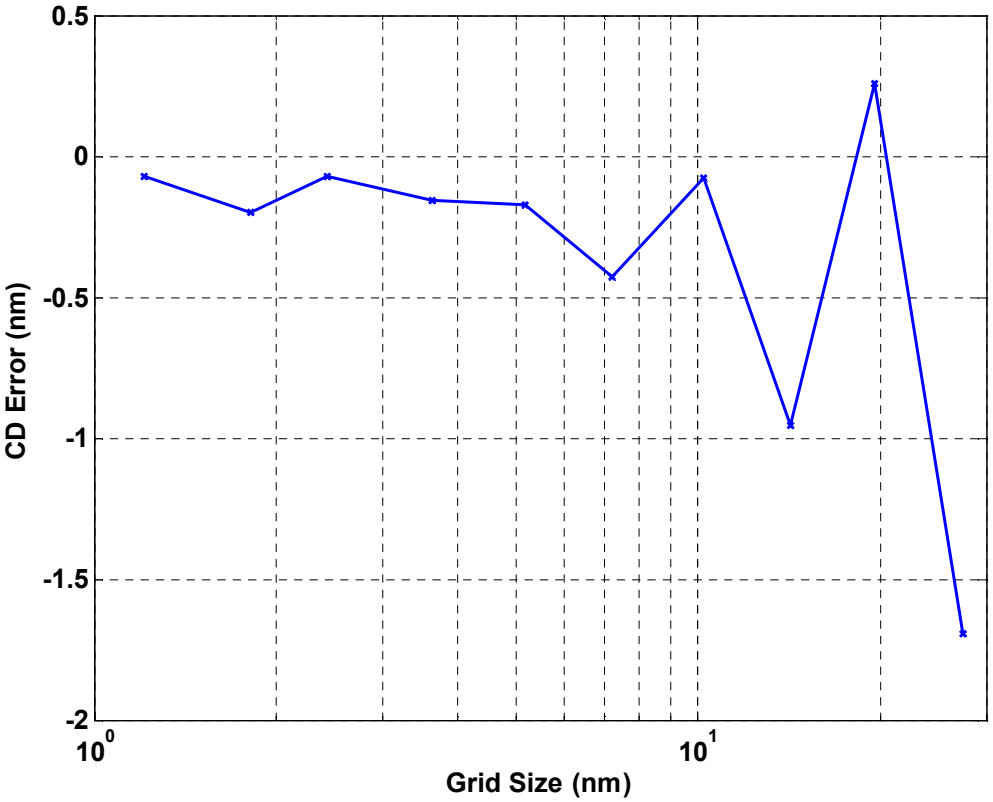

Figure 6. CD error vs. grid size for an exponential develop rate in y with parameters R_0 = 5.0 nm/s and γs = *0.038nm*$^{-1}$.

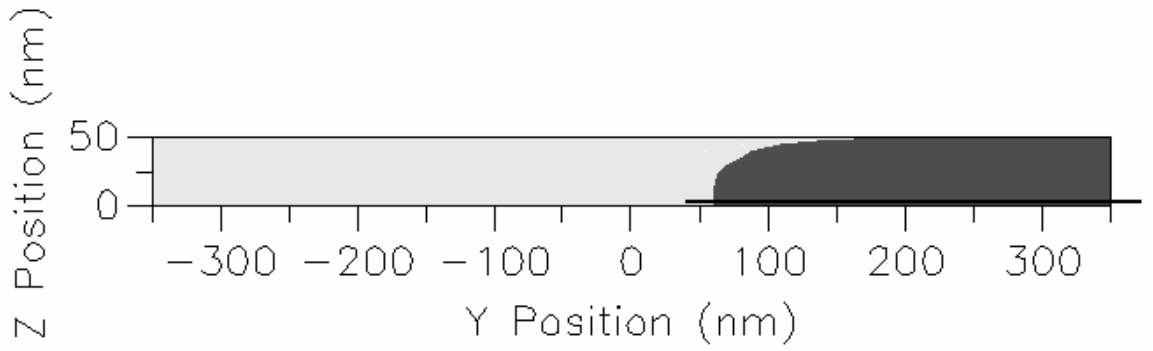

Figure 7. Resist profile and CD metrology plane (horizontal line) for an exponential develop rate with R_0 = 5.0 nm/s and $\gamma s = 0.038nm^{-1}$.

4. CONCLUSION

We have found closed form solutions for PEB and develop models. In the case of PEB, an analytic solution was found for the latent image after PEB for 2-beam, coherent illumination, with no quencher in the resist. PROLITH's PEB method converges rapidly to the exact solution.

For development, we derived two analytic solutions, one for a linear develop rate and another with an exponential develop rate. PROLITH's develop method gave good results against these closed-form test cases. Good convergence was seen for a non-realistic (but analytically solvable) linear develop rate. Sub-nanometer accuracy and very good convergence in the more realistic exponential develop rate was observed.

5. REFERENCES

1. M.D. Smith, C.A. Mack, "Methods for Benchmarking Photolithography Simulators", *Proc. SPIE*, Vol. 5040 (2003) pp. 57-68.
2. M.D. Smith, J. D. Byers, C.A. Mack, "Methods for Benchmarking Photolithography Simulators: Part II", *Proc. SPIE,* Vol. 5377 (2004) pp. 1475-1486.
3. Mark D. Smith, Trey Graves, Jeffrey D. Byers, Chris A. Mack, "Methods for Benchmarking Photolithography Simulators: Part III," *Optical Microlithography XVIII, Proc*., SPIE Vol. 5754-99 (2005).
4. T. Brunner, "SEMATECH Report: Benchmark tests for image simulation programs used in optical lithography", SEMATECH (1994).
5. R.L. Gordon, "Exact Computation of 2D Aerial Imagery," *Proc. SPIE*, Vol. 4692 (2002) pp. 517-528.
6. M.D. Smith, J. D. Byers, C.A. Mack, "The lithographic impact of resist model parameters", *Proc. SPIE,* Vol. 5376 (2004) pp. 322-332.
7. Hinsberg, et al. "Extendibility of chemically amplified resists: another brick wall?", *Proc. SPIE*, Vol. 5039 (2003) pp. 1-14.
8. Abramowitz, M. and Stegun, I. A. (Eds.). "Modified Bessel Functions I and K." §9.6 in Handbook of Mathematical Functions with Formulas, Graphs, and Mathematical Tables, 9th printing. New York: Dover, pp. 374-377, 1972.
9. Donald R. Smith, Variational Methods in Optimization, Dover Publications, Inc. (Mineola, NY: 1974).
10. C. A. Mack, "PROLITH: A Comprehensive Optical Lithography Model," *Optical Microlithography IV, Proc.*, SPIE Vol. 538 (1985) pp. 207-220.
11. J. D. Byers, M. D. Smith, and C. A. Mack, "Lumped Parameter Model for Chemically Amplified Resists," *Optical Microlithography XVII, Proc*., SPIE Vol. 5377 (2004) pp. 1462-1474.